21, rue d'Artois, F-75008 PARIS
http : //www.cigre.org

CIGRE US National Committee
2022 Grid of the Future Symposium

Virtual Synchronous Generator Controller Performance and Evaluation

M.M. BADRELDIEN, B.K. JOHNSON
University of Idaho
USA

SUMMARY

Distributed energy resources such as wind and photovoltaic are adopted in many parts of the world to control greenhouse gases. The controls for these resources are designed as if they are connected to a stiff power system. However, the high penetration of these renewable resources, with commonly used converter control schemes, offsetting the operation of the conventional synchronous generators in the grid diminishes the total system inertia and so affects the system stability. This problem is more evident in small systems when a large utility grid is not available. To solve this problem, the converters combined with energy storage systems connected to these resources can mimic the inertial features of the conventional synchronous generator which is referred to as a virtual synchronous generator. This increases the total system inertia, enhances the system stability and operation at different disturbances, and provides support to the power grid.

This paper starts by describing the model and design of a virtual synchronous generator, then its operation in different scenarios to verify its features. Moreover, it describes how the inertia and damping constants affect the system performance against different disturbances. Furthermore, the effects of inertia and damping constants on the energy storage system are described. The system has been modeled and simulated using electromagnetic transient simulation.

KEYWORDS

Virtual synchronous generator, inertia emulation, power converter, power system stability

badr6124@vandals.uidaho.edu

1. INTRODUCTION

Renewable energy resources (RERs) such as wind, solar photovoltaic (PV), and fuel cells usually supply electric power to the utility grids through power electronic converter interfaces. Compared with the conventional synchronous generators (CSGs), RERs don't have rotor intrinsic kinetic energy (mechanical inertia). The applications of these RERs are expanding in the electric power system and it is expected to be increased more and more in the future.

Connecting the RERs with the low or zero inertia in the power system drastically reduces the overall system inertia, especially if they offset conventional synchronous generation. Hence, the power system stability and its dynamic performance are negatively affected. To obtain a decent power system performance, the converters have to be well designed and controlled. The power system operation and its dynamics performance depend on the converter controllers and their operation methodologies.

Traditional droop methods have been used to control the converters and share their output power by controlling the output voltage magnitude and frequency according to their output active and reactive power. Also, the controllers try to mimic the droop characteristics of the CSGs [1].

Additional research work has been developed to mimic the steady-state droop characteristics and the dynamic characteristics of the CSGs to enhance the inertia of the system. Virtual synchronous generator (VSG) and virtual inertia (VI) emulation approaches have been proposed as solutions to integrate the RERs into the power system and enhance the system inertia. With energy storage systems (ESSs), the converters will be able to supply or absorb abrupt power fluctuations and mimic the kinetic energy in CSG to provide inertia. Moreover, VSG converters will move from just grid following to grid supporting and grid forming converters. Hence, VSG methodologies enhance the stability and dynamic performance of renewable energy generators. Moreover, the power electronic converters can provide ancillary services such as voltage regulation and help to improve the stability of the power system.

VSG development underwent several research steps over the last years. The first control method was introduced by Beck and Hess in [2]. It was called a virtual synchronous machine (VISMA). The authors tried to emulate CSG features and provide virtual inertia to increase the system inertia and support its stability.

This concept was embraced by many authors later with different characteristics and operation methodologies. The authors of [3]-[5] adopted current source-controlled VSG converters. This category is applicable for grid-connected systems with a low renewable energy resources penetration. The authors proposed virtual synchronous machines to enhance the system inertia and support its stability.

The second category is the voltage source-controlled VSG converter. This type of VSG is applicable for both grid-connected and isolated modes of operations. The authors of [6]-[8] proposed synchroverters that work as voltage-source VSG converter controllers to emulate the CSG inertia.

In this paper, the inertial features and damping constants of the CSG are emulated in VSG. This can enhance the system's performance and support its frequency against different disturbances. Furthermore, the converter can work with the hierarchical control levels and may receive its reference set values from the different controllers. The converter is connected to a battery energy storage system to supply the required power. The models for different subsystems are described including the converter controllers' outer and inner loops that mimic the CSG, and the system is modeled using an electromagnetic transient simulation program to verify the proposed controller.

The rest of this paper is arranged as follows. Section 2 describes the layout of the system. In Section 3 the VSG controller structure is presented including inertial emulation, voltage controller, and inner loop controllers. Section 4 describes the energy storage system and its controller. The simulation of the proposed system is presented in Section 5. Finally, in Section 6, some relevant conclusions are drawn.

2. SYSTEM LAYOUT

Fig. 1 describes the proposed system in which the PV is the primary source of electric power. The dc-dc boost converter is used to step up the PV output voltage and maximize the energy extracted from the PV array.

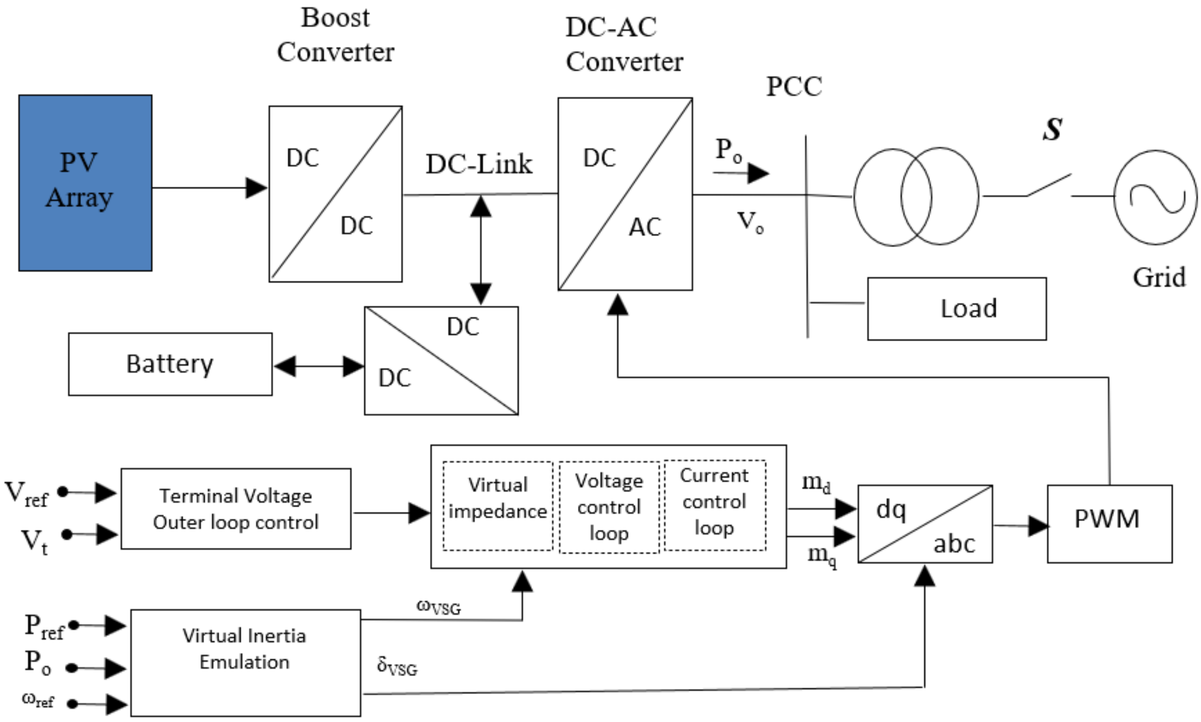

Fig. 1. General layout of the proposed system

Modeling of the PV array and its converter is well described in [9]-[11]. The DC-AC converter is used to connect the power from the dc-link to the grid that is simulated by a voltage source. An energy storage system is required to emulate the CSG features, so a battery storage system is used to supply the required power and energy to the system through a bidirectional buck-boost converter. DC-AC converter controller consists of two main loops, outer and inner loops. The outer loops consist of two main parts. The first part is the virtual inertia emulation part, it generates the virtual load angle. The second part is the terminal voltage control part, it generates the reference signals to the inner control loops. The inner control loops consist of two cascaded voltage and current control loops to generate the signals that drive the switches. In the following subsections, an explanation and the mathematical model of the parts of the system will be described.

3. VSG CONTROLLER STRUCTURE

A. Inertial Emulation of VSG

The main objective of VSG is to emulate the main behavior of conventional synchronous generators by controlling the power converter. Moreover, the model of VSG is an arbitrary design choice to determine what is modeled from the CSG. If the purpose of the VSG is to accurately replicate the CSG, then the fifth-order electrical model and the second-order mechanical model have to be modeled in VSG [3]. Although the full order model matches the behavior of CSG, it adds unnecessary complexity if the purpose of VSG is to emulate the inertial and damping properties of CSG since the inertial response and damping are the essential features in the VSG. Furthermore, the transient and sub-transient dynamics are included or excluded based on the required degree of complexity and accuracy.
The inertia and damping constants that are emulated in this paper can be described by the swing equation of the conventional SG which can be derived from Newton's Law of Motion for rotating objects, it can be written as [3],[12]:

$$T_m - T_e - D(\omega - \omega_g) = J(d\omega/dt) \quad (1)$$

where T_m is the mechanical torque driving the generator, T_e is the electromagnetic torque due to electric load on the generator, D is the coefficient accounting for the damping torque associated with the damper winding, ω is the rotational speed of the machine, ω_g is the grid frequency, J is the rotor inertia.
It has to be mentioned that the coefficient D in the SG is not constant for all operating points, and it depends on the operating point. So a fixed value of D in the simplified model for representing the main features of CSG will not be able to match the CSG behavior in all operating ranges.
The swing equation can be written in terms of power instead of torque by multiplying the equation (1) by frequency ω. For a small oscillation around the synchronous speed, the power balance may be described in the Laplace domain by the approximation given by:

$$P_m - P_e - K_d(\omega - \omega_g) \approx J\, \omega_g S\ \omega \quad (2)$$

where P_m is the emulated mechanical input power, P_e is the electrical output power, and K_d is the damping constant associated with the constant D. Equation (2) can be expressed in per unit as:

$$P_m - P_e - K_d(\omega_{pu} - \omega_{gpu}) \approx T_a\ \omega_{pu} S \quad (3)$$

where the time constant $T_a = 2H$, H is the per unit inertia constant for the stored kinetic energy in the rotor at rated speed divided by the chosen MVA base. The block diagram describing the swing equation is shown in Fig. 2. The active power is associated with the VSG emulated torque and angular speed of the rotor. The virtual rotor angle δ_{VSG} generated from Fig. 2 emulates the phase angle of the voltage induced by VSG and it is used in the Park's transformation and the inner loops on the converter controllers.

B. Voltage Controller

The voltage magnitude of VSG can be controlled by a decoupled voltage or reactive power control loop. Controlling the terminal voltage enables the converter to operate in both grid-connected and isolated modes of operation. Fig. 3 describes the voltage control outer loop that generates the voltage control signals. The reference voltage is aligned to coincide with the direct axis of the converter voltage reference frame and the quadrature axis voltage is set to zero.
The reference signals are passed through a virtual impedance. The virtual parameters R_v and L_v are used to emulate the stationary impedance in the synchronous generator. It can stabilize the VSG against small disturbances in the system. The virtual impedance block diagram is shown in Fig. 4. The control signals ($V_{d\text{-}set}$ and $V_{q\text{-}set}$) generated from Fig. 4 are used as the input reference signals to the cascaded inner voltage and current control loops.

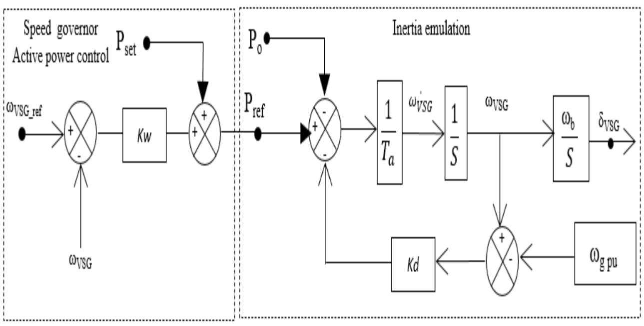

Fig. 2. Virtual inertia emulation

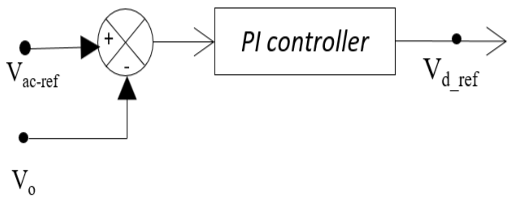

Fig. 3. Voltage controller

C. Inner Control Loops

The inner control loops consist of two cascaded voltage and current control loops. The first voltage control loop generates the reference current signals to the second current loop. These current signals are controlled against over current due to abnormal conditions. The second current control loop controls the current to follow its reference values. The inner cascaded loops are shown in Fig. 5. The system has been modeled in a synchronously rotating dq reference frame.

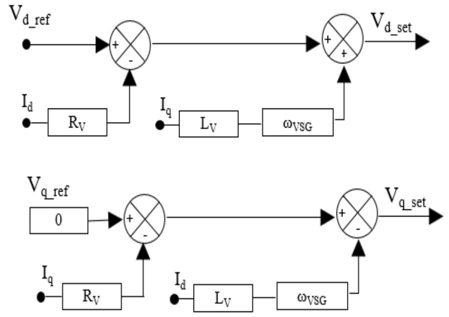

Fig. 4. Virtual impedance

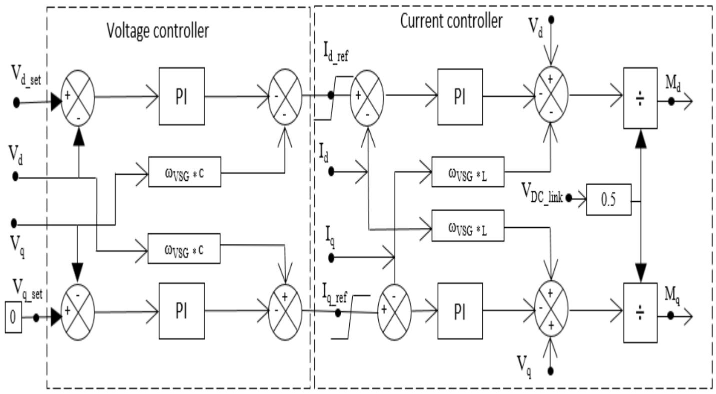

Fig. 5. Cascaded voltage and current control loops

4. ENERGY STORAGE SYSTEM

The model of the battery can be described by a non-linear equation and the battery is modeled using a controlled voltage source connected to a series resistance as shown in Fig. 6. The open voltage source *E* is calculated by using a non-linear equation based on the actual battery state of charge. The generic battery model equation can be written as [11]:

$$E=E_o - K(Q/(Q-it))+A.e^{(-B.\int idt)} \quad (4)$$

$$V_b = E-R_i*i \quad (5)$$

where *E* is no load voltage source controller (V), E_o is a battery constant voltage (V), *Q* is the battery's capacity (Ah), *K* is polarization voltage constant (V), the integral $\int i\,dt$ represents the actual battery charge (Ah), *B* is the exponential constant inverse capacity $(Ah)^{-1}$, *A* is exponential voltage zone amplitude (V), R_i is the battery internal resistance (Ω), V_b is the battery terminal voltage (V) and *i* is the battery current (A). A detailed explanation of the battery model is described in [13].

A bidirectional dc-dc buck-boost converter (BDBBC) is used to control the operation of the battery. The converter operates in both buck and boost modes based on the dc-link voltage magnitude. It tries to keep the value of the dc-link constant. It works on the buck mode when the battery is charging. On the contrary, the converter works on the boost mode to discharge the battery to meet the load demands. Fig. 7 shows the schematic diagram of the converter which consists of two main switches S_1 and S_2 that enable the battery to charge or discharge. A complete explanation of the BDBBC and its controller is described in [13],[14].

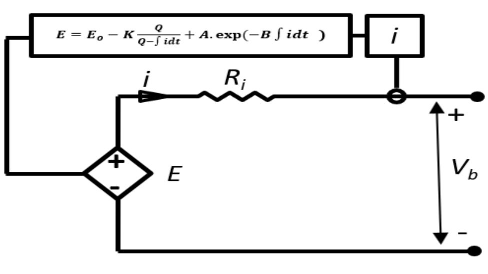

Fig. 6. Equivalent circuit of the battery

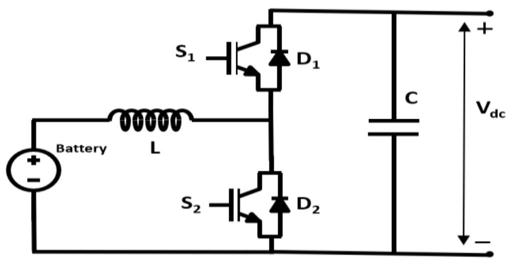

Fig. 7. Battery buck-boost converter

5. SIMULATION RESULTS

The system shown in Fig. 1 is implemented and modeled with an electromagnetic transients program to verify the proposed control structure. Different cases are carried out to describe the features and capabilities of the VSG.

Fig. 8 describes the first case with a change in the reference power to the converter. This change may be set by the local or hierarchical level controllers in response to a sudden change in the load or generated power from the PV array or on the local power subsystem. It can be shown that the converter's output power follows its reference, and the output power profile depends on the value of the inertial time constant. When the inertial time constant increases, the system has a larger amplitude power oscillation. This change affects the mechanical virtual frequency of the VSG. The frequency profile is shown in Fig. 9, it can be shown that when the inertia time constant decreases, the frequency change is more profound. Also, it has a higher rate of change.

The difference between the converter output power and the PV generated power is compensated by the battery system. Fig. 10 describes the battery power, it can be shown that when the inertia time constant increases, the battery power increases. So, the energy storage system power design and rating should be based on the emulated inertia constants.

The next set of simulations describes the effect of damping constant change on the VSG operation. Fig. 11 describes the output power profile at different damping constants. It is shown that increasing the damping constant reduces the amplitude of power oscillations, and the system reaches its steady state sooner. Moreover, the frequency is improved as shown in Fig. 12 such that the frequency nadir is decreased when the damping constant increases.

Fig. 13 describes the battery power, it can be shown that the battery power is decreased when the damping constant increases. So the size of the battery system connected with the VSG is affected by the emulated inertia and damping constants. Fig. 14 and Fig. 15 describe how the battery storage power changes with the emulated inertia and time constants.

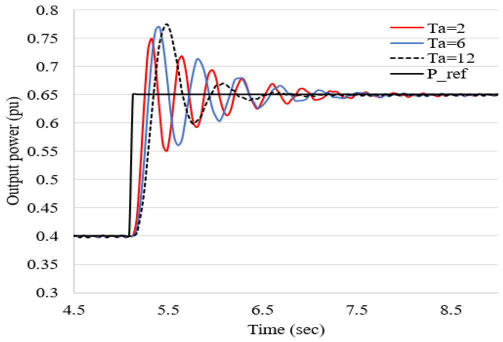

Fig. 8. VSG active power variation at different inertia time constants

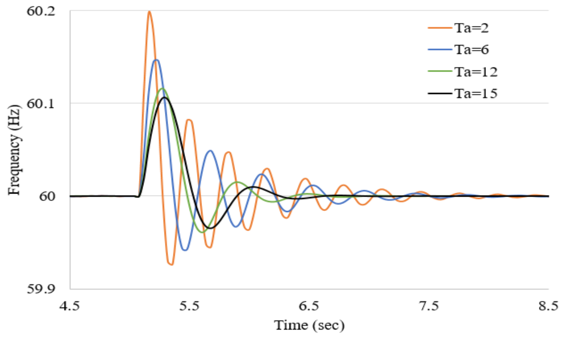

Fig. 9. Frequency profile at different inertia time constants

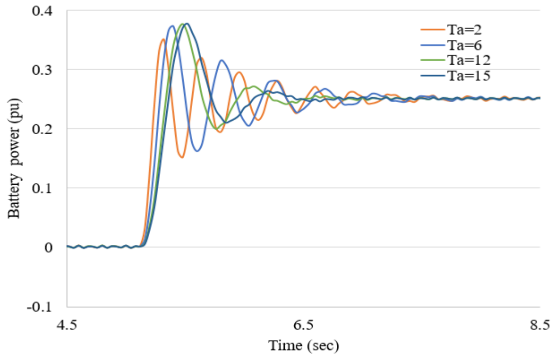

Fig. 10. Battery power at different inertia time constants

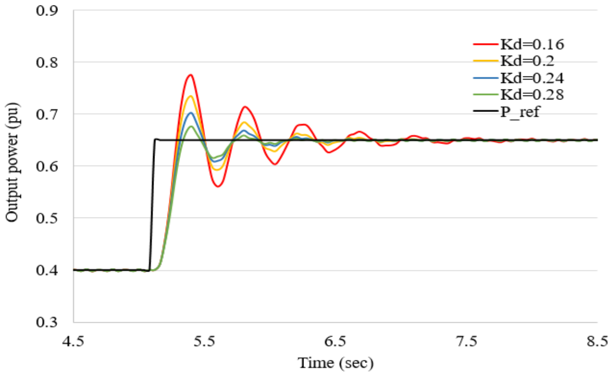

Fig. 11. VSG active power variation at different damping constants

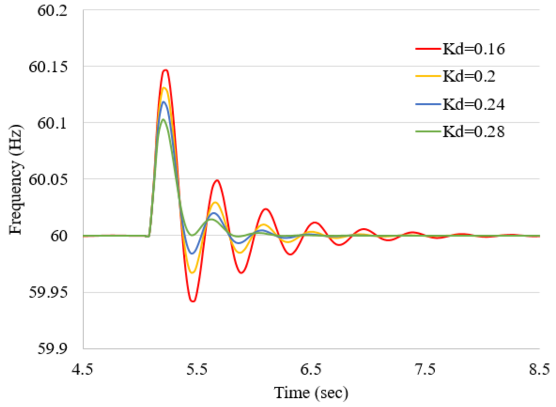

Fig. 12. Frequency profile at different damping constants

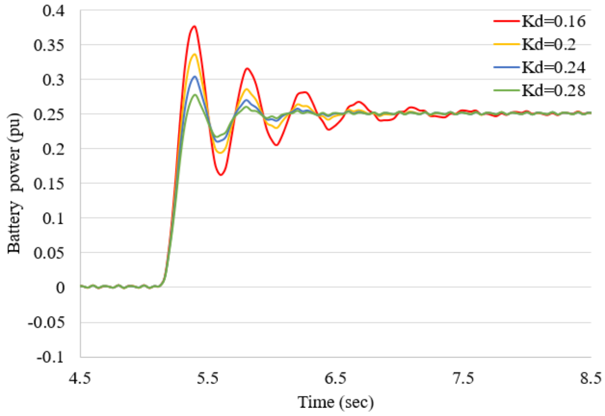

Fig. 13. Battery power at different damping constants

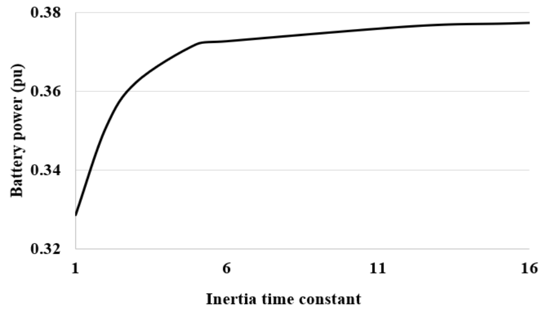

Fig. 14. Battery power variation with respect to the inertia time constant

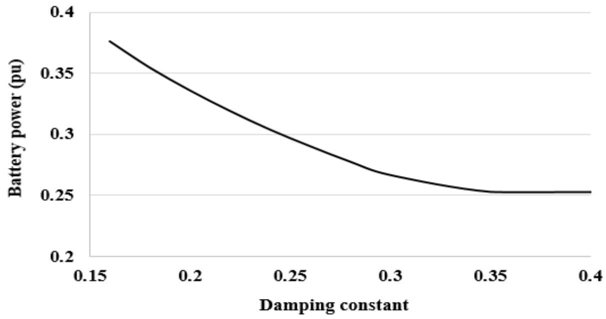

Fig. 15. Battery power variation with respect to damping constant

The next set of simulations describes the response of the system to a sudden 0.3 pu increase in load. It can be shown from Fig. 16 that the high inertial system can supply more inertial power when a sudden load is added to the system. Moreover, as shown in Fig. 17 the high inertial system has a slower rate of frequency change and smaller frequency nadir.

The previous simulation case is repeated at different damping constants. Fig. 18 and Fig. 19 describe the converter output power and frequency respectively when the load is increasing by 0.3 pu. It can be seen that increasing the damping constant helps the system to reach the steady state sooner and reduces the frequency oscillations.

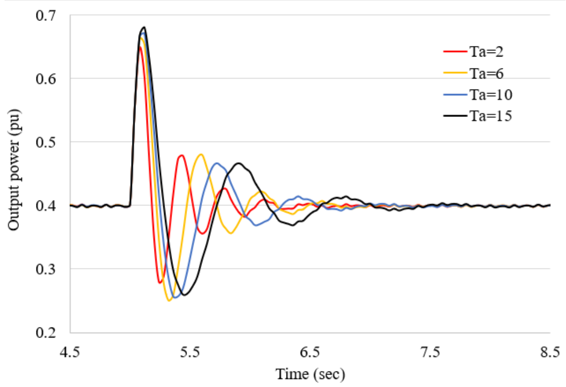

Fig. 16. VSG active power variation at different inertia time constants

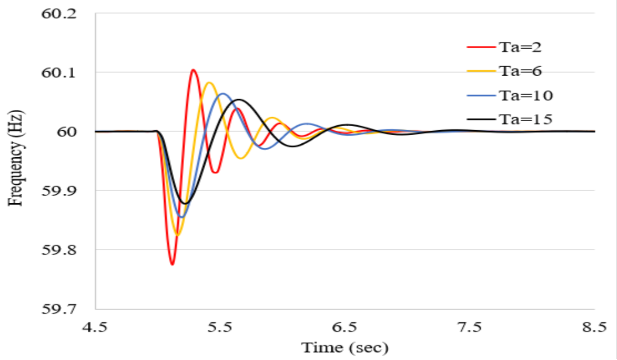

Fig. 17. Frequency profile at different inertia time constants

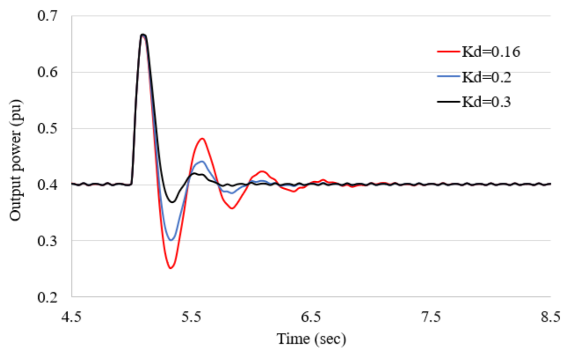

Fig. 18. Output power profile at step increase in load

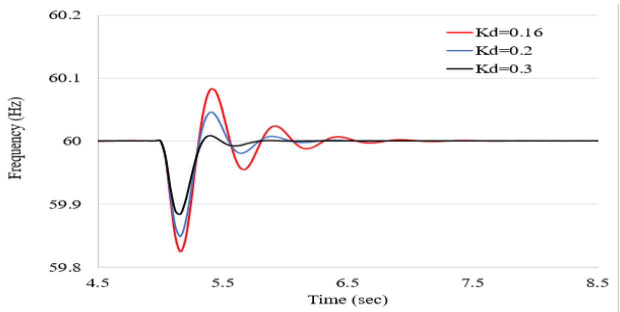

Fig. 19. Frequency profile at step increase in load

The next simulation set describes how the VSG responds to the change in the system frequency. The system frequency decreased at a time equal to 5 sec from 60 Hz to 59.6 Hz due to an external event elsewhere in the microgrid as shown in Fig. 20. The system is simulated at different inertia time constants. The VSG supplies inertial power in response to the frequency change. The high inertial system supplies instantaneous more inertial power than the lower inertial system as shown in Fig. 21. The output power reaches a higher steady state output power due to the droop effect of the virtual emulated governor.

The previous simulation case is repeated at different damping constants. Fig. 22 describes the frequency drops from 60 Hz to 59.6 Hz and Fig. 23 describes the converter output power. It can be seen that increasing the damping constant reduces the maximum amplitude of the output power oscillations and helps the system to reach a steady state sooner.

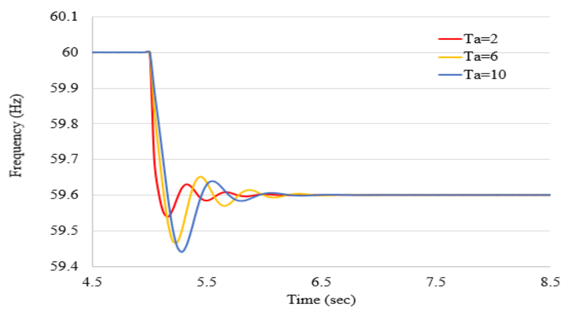

Fig. 20. VSG frequency change in response to a microgrid frequency change

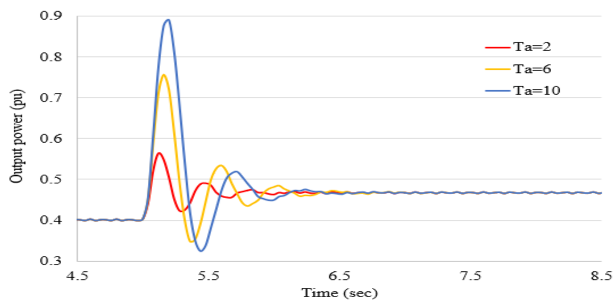

Fig. 21. Output power in response to a microgrid frequency change

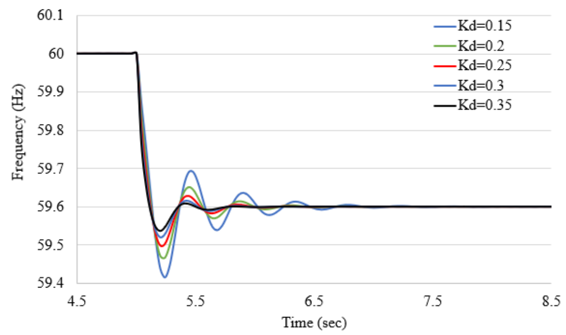

Fig. 22. VSG frequency change in response to a microgrid frequency change

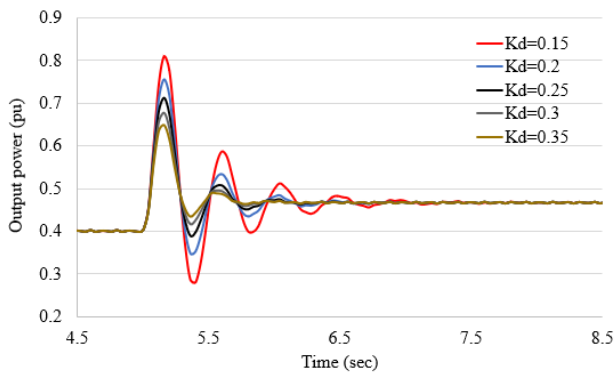

Fig. 23. Output power in response to a microgrid frequency change

The change in the steady state output power in Fig. 21 and Fig. 23 is due to the droop effect in the governor model. To describe the inertial effect only the droop constant is set to equal to zero and the test has been repeated. Fig. 24 describes the output power profile at different inertia time constants. It

can be seen that the high inertia system can supply more inertial power when the system frequency changes and thus needs a battery and associated converters with higher power ratings.
The simulation case is repeated at different damping constant, Fig. 25 describes the output power profile when the grid frequency changes from 60Hz to 59.6 Hz at a time equal to 5 sec. It is shown that increasing the damping constant reduces the converter output power and the system can reach its steady state sooner.

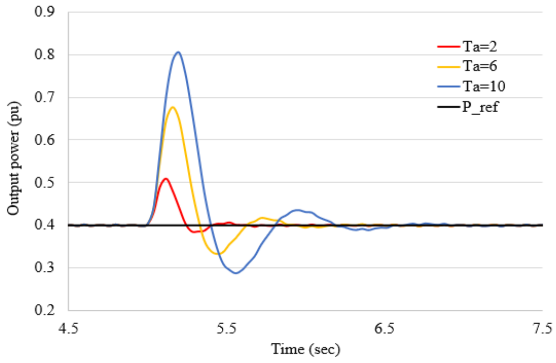

Fig. 24. Output power in response to a microgrid frequency change

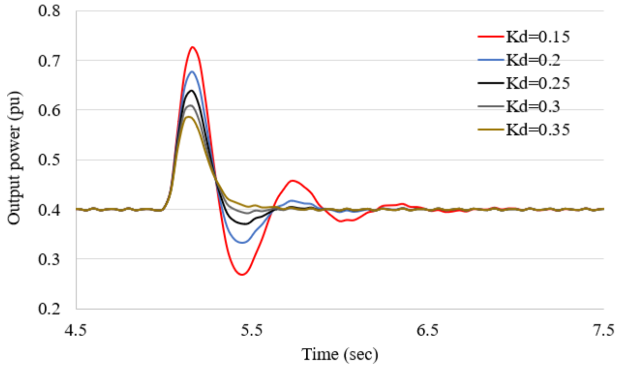

Fig. 25. Output power in response to a microgrid frequency change

6. CONCLUSION

The stability of the system is impacted by the total system inertia which is affected by the number of conventional synchronous generators and renewable energy resources connected to the grid. The concept of VSG as a technique to control the power converter to mimic the inertial features of CSG has been described in this paper. The implementation of VSG in the paper is based on the swing equation to generate the reference control signals to the converter's inner control loops. Also, the model for VSG has been described in a synchronously rotating reference frame. The whole system including the PV array, ESS, and power converters is implemented using an electromagnetic transient program.
From the simulation results, it can be concluded that the power converter combined with ESS can emulate the inertial features of CSG. Moreover, the parameters of VSG can be changed to mimic the inertial features of many synchronous generators. Furthermore, the ESS depends on the emulated inertia and damping constants, such that when the inertia constant increases or the damping constant decreases, the ESS power capability has to be increased, and vice versa. Moreover, when the inertia and damping constants increase, the frequency oscillation is reduced which helps to stabilize the system against different disturbances.
Finally, the power converter based on VSG techniques helps to increase the dependency on RERs and spread them in the power grids.

BIBLIOGRAPHY

[1] M. Dreidy, H. Mokhlis, and S. Mekhilef, “Inertia response and frequency control techniques for renewable energy sources: A review,” Renewable and sustainable energy reviews, vol. 69, pp. 144–155, 2017.
[2] H.-P. Beck and R. Hesse, “Virtual synchronous machine,” in 2007 9th International Conference on Electrical Power Quality and Utilisation. IEEE, 2007, pp. 1–6.
[3] S. D’Arco and J. A. Suul, “Virtual synchronous machines—classification of implementations and analysis of equivalence to droop controllers for microgrids,” in 2013 IEEE Grenoble Conference. IEEE, 2013, pp. 1–7.
[4] T. Loix, “Participation of inverter-connected distributed energy resources in grid voltage control (deelname van omvormergekoppelde gedis-tribueerde energiebronnen aan de regeling van de netspanning),” 2011.

[5] Y. Chen, R. Hesse, D. Turschner, and H.-P. Beck, “Improving the grid power quality using virtual synchronous machines,” in 2011 International conference on power engineering, energy and electrical drives. IEEE, 2011, pp. 1–6.
[6] Q.-C. Zhong and G. Weiss, “Synchronverters: Inverters that mimic synchronous generators,” IEEE transactions on industrial electronics, vol. 58, no. 4, pp. 1259–1267, 2010.
[7] J. Liu, Y. Miura, and T. Ise, “Comparison of dynamic characteristics between virtual synchronous generator and droop control in inverter-based distributed generators,” IEEE Transactions on Power Electronics, vol. 31, no. 5, pp. 3600–3611, 2015.
[8] M. Abuagreb, B. Ajao, and B. K. Johnson, “Implementation of emulated inertia using PV generation with energy storage to improve integrated grid response,” in 2020 IEEE Texas Power and Energy Conference (TPEC). IEEE, 2020, pp. 1–6.
[9] M. Abuagreb, A. Abuhussein, and S. AlZahir, “Sizing of energy storage system for virtual inertia emulation,” arXiv preprint arXiv:2201.06566, 2022.
[10] M. M. Badreldien, M. Abuagreb, M. F. Allehyani, and B. K. Johnson, “Modeling and control of solar PV system combined with battery energy storage system,” in 2021 IEEE Electrical Power and Energy Conference (EPEC). IEEE, 2021, pp. 373–377.
[11] M. Abuagreb, M. Allehyani, and B. K. Johnson, “Design and test of a combined PV and battery system under multiple load and irradiation conditions,” in 2019 IEEE Power & Energy Society Innovative Smart Grid Technologies Conference (ISGT). IEEE, 2019, pp. 1–5.
[12] O. Beltran, R. Peña, J. Segundo, A. Esparza, E. Muljadi, and D. Wen- zhong, “Inertia estimation of wind power plants based on the swing equation and phasor measurement units,” Applied Sciences, vol. 8, no. 12, p. 2413, 2018.
[13] M. Abuagreb, H. Beleed, and B. K. Johnson, “Energy management of a battery combined with PV generation,” in 2019 North American Power Symposium (NAPS). IEEE, 2019, pp. 1–6.
[14] M. Abuagreb, M. Allehyani, and B. K. Johnson, “Design and test of a combined PV and battery system under multiple load and irradiation conditions,” in 2019 IEEE Power & Energy Society Innovative Smart Grid Technologies Conference (ISGT). IEEE, 2019, pp. 1–5.